Dalton Transactions

COMMUNICATION

Ferritin Encapsulation of Artificial Metalloenzymes: Engineering a Tertiary Coordination Sphere for an Artificial Transfer Hydrogenase

Received 00th January 20xx,
Accepted 00th January 20xx

DOI: 10.1039/x0xx00000x

www.rsc.org/

Martina Hestericová, [a] Tillmann Heinisch, [a] Markus Lenz [b] and Thomas R. Ward*[a]

Ferritin, a naturally occuring iron-storage protein, plays an important role in nanoengineering and biomedical applications. Upon iron removal, apoferritin was shown to allow the encapsulation of an artificial transfer hydrogenase (ATHase) based on the streptavidin-biotin technology. The third coordination sphere, provided by ferritin, significantly influences the catalytic activity of an ATHase for the reduction of cyclic imines.

Biocatalysis is an attractive means to prepare high-added value products under environmentally benign conditions. Over the past few decades, the use of biocatalysis has expanded significantly and is now widely applied for the synthesis of chemicals, pharmaceuticals, fragrances etc.[1] To expand the biocatalytic repertoire, artificial metalloenzymes[2] (ArMs hereafter) have attracted increasing attention.[3]

ArMs, that result from the incorporation of an organometallic moiety within a protein or DNA scaffold, combine attractive features of both enzymatic and homogeneous transition metal catalysis.[3,4] To ensure the localization of the cofactor within the scaffold, the biotin-streptavidin technology (biot-Sav hereafter) has found widespread use.[5] The protein scaffold provides a well-defined second coordination sphere around the metal moiety, and interacts with the cofactor, the substrates and intermediates. Accordingly, it significantly affects the selectivity and reaction rate of the ArM.[6]

Inspection of the X-ray structures of various ArM based on the biot-Sav technology reveal that the biotinylated cofactor is partially solvent-exposed.[7] Efforts to genetically engineer the biotin-binding vestibule by introduction of various extended loops has shown promise.[8] Building on our experience with mineralizing ArMs within silica nanoparticles,[9] we reasoned that one may encapsulate an ATHase[10] within a hollow protein shell. This additional protein environment, which provides a tertiary coordination sphere to the ArM[11] was anticipated to influence the catalytic activity, both in terms of activity and selectivity.

Inspection of the size of homotetrameric Sav (4.5 nm · 5.5 nm · 5.1 nm) led us to hypothesize that ferritin (from horse spleen, inner diameter 7-8 nm) may offer an ideal capsule to host an ArM (Figure 1).

Fig 1. Apoferritin (indigo cartoon display, PDB code: 5c6f) offers a commensurate hollow to encapsulate an artificial metalloenzyme based on the biotin-streptavidin technology (Sav, magenta cartoon display, the [Cp*Ir(biot-*p*-L)Cl] cofactor, blue, is displayed as

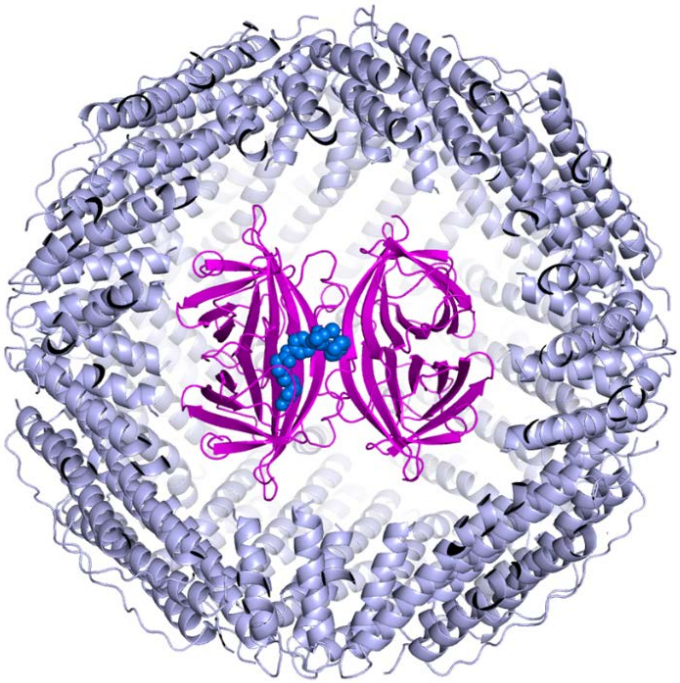

space-filling; PDB code: 3pk2). The model was generated by manually docking the ATHase within apoferritin.

[a] *Department Chemistry, University of Basel, Mattenstrasse 24a, BPR 1096, Basel, 4002 (Switzerland) e-mail: thomas.ward@unibas.ch.*
[b] *Institute for Ecopreneurship, School of Life Sciences, University of Applied Sciences and Arts Northwestern Switzerland, Gründenstrasse 40, Muttenz, 4132 (Switzerland).*
Electronic Supplementary Information (ESI) available. See DOI: 10.1039/x0xx00000x

Herein, we report on our efforts to compartmentalize an ATHase based on the biotin-streptavidin technology within apoferritin.[12]

Building on our experience with ATHase relying on the [Cp*Ir(biot-*p*-L)Cl] cofactor,[13] we set out to encapsulate the preassembled ArM [Cp*Ir(biot-*p*-L)Cl]·Sav within the cavity of horse spleen apoferritin. The following Sav mutants pre-assembled with the biotinylated iridium catalyst were selected for encapsulation: [Cp*Ir(biot-*p*-L)Cl]·S112A Sav (an (*R*)-selective imine reductase), [Cp*Ir(biot-*p*-L)Cl]·S112K Sav (an (*S*)-selective imine reductase) and [Cp*Ir(biot-*p*-L)Cl]·K121A-S112A Sav (the most active imine reductase based on the biot-Sav complex).[9,13a] The ATHase was encapsulated within ferritin (ATHase@ferritin) by disassembling apoferritin upon decreasing the pH < 2.[14] Upon increasing the pH to 8, the quaternary structure of ferritin is restored, thus allowing to encapsulate cargoes that are commensurate with the inner diameter of apoferritin. This strategy has been used to encapsulate various small molecules, nanoparticles, nanocrystals etc.[15] To the best of our knowledge however, this approach has not been used to encapsulate proteins within apoferritin.

To highlight the encapsulation of Sav upon reassembly of the ferritin cage, we selected Sav equipped with one equivalent of a fluorescent biotinylated probe per four free biotin binding sites (fbs) of Sav. Accordingly, Sav S112A (tetramer, containing four fbs) was preincubated with one equivalent of biotin-4-fluorescein (B4F hereafter) and added to apoferritin at pH = 2 (i.e. disassembled apoferritin). Upon increasing the pH to 8, B4F·Sav S112A is encapsulated within ferritin (B4F·Sav S112A@ferritin hereafter). To remove the unspecifically adsorbed B4F·Sav S112A from the outer-surface of apoferritin, the solution was treated at pH = 8 with iminobiotin-sepharose beads and washed extensively. The iminobiotin moiety binds to free biotin-binding sites present in B4F·Sav S112A, thus allowing to remove B4F·Sav S112A that is not encapsulated within apoferritin by means of centrifugation and filtration. The solution that contains B4F·Sav S112A@ferritin was then subjected to preparative size-exclusion chromatography (SEC).

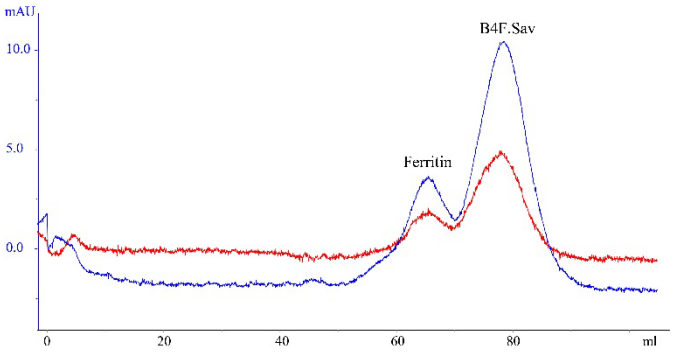

Fig 2. Preparative size-exclusion chromatogram of B4F·S112A-K121A Sav@ferritin. The blue line indicates absorbance at 280 nm. The absorbance at 495 nm (red trace) shows that B4F co-elutes with the apoferritin cage at 65 mL (run in 50 mM Tris-HCl, 100 mM NaCl, pH 8.0).

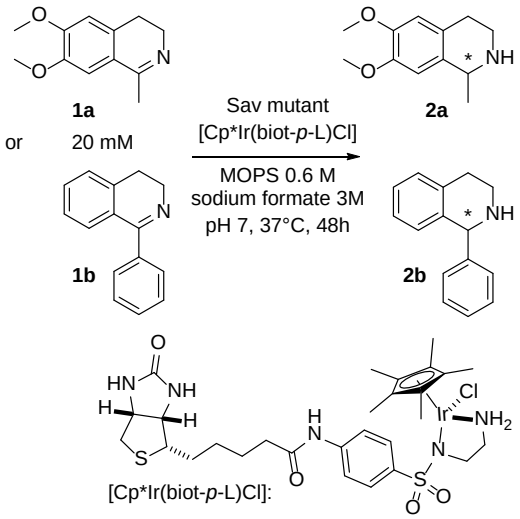

Scheme 1. Reduction of cyclic imines **1a** and **1c** using the ATHase.

Fluorescence analysis of the ferritin band unambiguously revealed the presence of B4F. As no fluorescence was detected upon adding B4F (instead of B4F·Sav) by means of size-exclusion chromatography (Figure S1), we hypothesize that B4F·Sav S112A@ferritin is formed (Figure 2).

Having highlighted the formation of B4F·Sav S112A@ferritin by fluorescence, we proceeded to encapsulate various ATHases in apoferritin following the same protocol. The resulting ATHases [Cp*Ir(biot-*p*-L)Cl]·S112A@ferritin, [Cp*Ir(biot-*p*-L)Cl]·S112K@ferritin and [Cp*Ir(biot-*p*-L)Cl]·S112A-K121A@ferritin were purified by preparative SEC (Figure S2). The presence of iridium in the purified Sav@ferritin samples was confirmed by means of ICP-MS. Upon sample digestion, the

Dynamic light scattering (DLS) measurements of the combined fractions containing the assembled ferritin shells revealed an increase in particle diameter of approx. 20% (Table S1). This observation suggests that the ATHase is indeed located within ferritin.

The presence of the ATHase within the ferritin cage [Cp*Ir(biot-*p*-L)Cl]·Sav@ferritin was further confirmed by comparison of the SDS- and native PAGE analysis. Under native conditions, the samples containing [Cp*Ir(biot-*p*-L)Cl]·Sav@ferritin revealed no band attributable to Sav (Figure S3). In contrast, under denaturing conditions, the Sav was released from the denatured ferritin cage and could be visualized by B4F on the SDS PAGE, as it contained two available fbs sites. Due to the remarkable stability of homotetrameric Sav, Sav maintained its tetrameric structure and biotin-binding activity, even under denaturing SDS PAGE conditions (Figure S4). In stark contrast, native PAGE analysis of a 1:1 mixture of [Cp*Ir(biot-*p*-L)Cl]·Sav and apoferritin revealed two bands (Figure S4, lane 5). This demonstrates that [Cp*Ir(biot-*p*-L)Cl]·Sav is encapsulated within ferritin, rather than unspecifically adsorbed on the outer-surface of ferritin, thus confirming the DLS observations.

Entry	Catalyst[a]	[Ir] (μM)	Sub.	ee (%)[b, c]	conv. (%)[b]	TON
1	[Cp*Ir(biot-*p*-L)Cl]	50	**1a**	*rac.*	16	65
2	[Cp*Ir(biot-*p*-L)Cl]	50	**1b**	*rac.*	18	71
3	[Cp*Ir(biot-*p*-L)Cl]·S112A	50	**1a**	75	35	142
4	[Cp*Ir(biot-*p*-L)Cl]·S112A	50	**1b**	43	39	154
5	[Cp*Ir(biot-*p*-L)Cl]·S112K	50	**1a**	-41	25	20
6	[Cp*Ir(biot-*p*-L)Cl]·S112K	50	**1b**	57	6	24
7	[Cp*Ir(biot-*p*-L)Cl]·S112A-K121A	50	**1a**	59	90	358
8	[Cp*Ir(biot-*p*-L)Cl]·S112A-K121A	50	**1b**	69	72	289
9	[Cp*Ir(biot-*p*-L)Cl]@ferritin	1.24[d]	**1a**	0	0.1	13
10	[Cp*Ir(biot-*p*-L)Cl]@ferritin	1.24[d]	**1b**	0	5	853
11	[Cp*Ir(biot-*p*-L)Cl]·S112A@ferritin	0.42[d]	**1a**	-46	0.2	74
12	[Cp*Ir(biot-*p*-L)Cl]·S112A@ferritin	0.42[d]	**1b**	24	5.6	2880
13	[Cp*Ir(biot-*p*-L)Cl]·S112K@ferritin	0.40[d]	**1a**	-47	0.1	46
14	[Cp*Ir(biot-*p*-L)Cl]·S112K@ferritin	0.40[d]	**1b**	24	5.6	2731
15	[Cp*Ir(biot-*p*-L)Cl]·S112A-K121A@ferritin	0.28[d]	**1a**	-44	0.2	117
16	[Cp*Ir(biot-*p*-L)Cl]·S112A-K121A@ferritin	0.28[d]	**1b**	20	5.6	3874
17	S112A-K121A@ferritin	0	**1a**	0	0	0
18	S112A-K121A@ferritin	0	**1b**	0	0	0
19	Apoferritin	0	**1a**	0	0	0
20	Apoferritin	0	**1b**	0	0	0
21	Apoferritin + [Cp*Ir(biot-*p*-L)Cl]·S112A-K121A	50	**1a**	55	85	340
22	Apoferritin + [Cp*Ir(biot-*p*-L)Cl]·S112A-K121A	50	**1b**	64	69	276
23	[Cp*Ir(biot-*p*-L)Cl]·S112A-K121A	1	**1a**	56	0.4	72
24	[Cp*Ir(biot-*p*-L)Cl]·S112A-K121A	1	**1b**	35	6	1108

[a] The reactions were performed using 20 mM substrate concentration at 37°C for 48 h (See Supplementary information for experimental details).[b] Enantiomeric excess and conversion were determined by HPLC analysis. [c] Positive ee values correspond to (*R*)-product and negative ee values correspond to (*S*)-product. [d] Values were calculated based on the [Ir] concentration determined by ICP-MS for each encapsulated ATHase batch.

Next, the encapsulated ATHases were tested for the reduction of cyclic imines **1a** and **1b** (Scheme 1). To determine the turnover number of the encapsulated ATHases (TON), ICP-MS analysis of samples containing Ir as [Cp*Ir(biot-*p*-L)Cl]·Sav@ferritin was carried out. The catalytic performance of the ATHases [Cp*Ir(biot-*p*-L)Cl]·Sav@ferritin was compared to the corresponding "free" ATHases: [Cp*Ir(biot-*p*-L)Cl]·Sav.

Since the isoquinoline substrates are protonated under the reaction conditions,[7d] they can penetrate through the ferritin 3-fold channels. In line with this assumption, we observed catalysis with all encapsulated ATHases.

All tested [Cp*Ir(biot-*p*-L)Cl]·Sav@ferritin, afforded preferentially (*S*)-**2a**. This contrasts with [Cp*Ir(biot-*p*-L)Cl]·Sav, which affords either (*R*)-**2a** or (*S*)-**2a**, depending on the Sav mutant: i) [Cp*Ir(biot-*p*-L)Cl]·Sav S112A affords **2a** in 75 % ee (*R)* and 35 % conversion (Table 1, entry 3) and [Cp*Ir(biot-*p*-L)Cl]·Sav S112K affords **2a** in 41 % ee (*S*) and 20 % conversion (Table 1, entry 5). Reduction of imine **1a** in the presence of the encapsulated [Cp*Ir(biot-*p*-L)Cl]·S112A Sav@ferritin affords (*S*)-**2a** in 46 % ee (*S*) (Table 1, entry 11).

Similarly, catalysis with [Cp*Ir(biot-*p*-L)Cl]·S112A-K121A Sav yields **2a** in 60 % ee (*R*) and 90 % conversion (Table 1, entry 7), while the encapsulated [Cp*Ir(biot-*p*-L)Cl]·S112A-K121A Sav@ferritin affords (*S*)-**2a** in 44 % ee (Table 1, entry 15). Control experiments with [Cp*Ir(biot-*p*-L)Cl]·S112A-K121A Sav at 1 μM catalyst loading afforded 56 % ee (*R*)-**2a** and 72 TON.

In the reduction of the less bulky **1b**, no inversion of enantioselectivity was observed in any of the tested encapsulated ATHases. However, the TONs have tripled with [Cp*Ir(biot-*p*-L)Cl]·S112A-K121A Sav@ferritin (entry 16) compared to the use of the free ATHase in buffer under similar conditions (entry 24). Similar TONs were also obtained for [Cp*Ir(biot-*p*-L)Cl]·S112A@ferritin, which afforded (*R*)-**2b** in 24 % ee and 2880 TON. The [Cp*Ir(biot-*p*-L)Cl]·S112K@ferritin afforded (*R*)-**2b** in 24 % ee and 2731 TON.

The effect on enantioselectivity and catalytic efficiency of the encapsulated ATHases depends on both the substrate and the used Sav mutant. Further studies in regards to the effect of point-mutations on the kinetic behavior of the hybrid catalysts are currently undergoing in our research group.

Overall, these findings highlight the influence of the third coordination sphere on the catalytic performance of the ferritin-encapsulated ATHases.

Taking advantage of the reversible dissociation and reassembly of apoferritin, we have compartmentalized an artificial metalloenzyme within a protein cage. The resulting ATHases maintained their catalytic activity, displaying up to > 3800 TON for the reduction of cyclic imines. The marked variation in enantioselectivity, observed upon ATHase encapsulation, highlights the combined effect of both the second- and third coordination sphere provided by Sav and ferritin respectively.

These results highlight the possibility to encapsulate an ArM within ferritin following a reassembly route. The significant improvement in TON compared to the free ArM suggests that this strategy may offer an attractive means to protect a precious metal in a cellular environment and possibly to deliver it *in vivo*, without eliciting an immune response.[16]

Conflicts of interest

There are no conflicts to declare.

Acknowledgements

This research was supported by the Swiss Nanoscience Institute (Project NanoZyme, DPA2238), the ERC (DrEAM) and the NCCR Molecular Systems Engineering. MRH would like to thank the Biophysics Facility of the University of Basel for the use of the DLS instrument.

References

1 (a) U. T. Bornscheuer, G. W. Huisman, R. J. Kazlauskas, S. Lutz, J. C. Moore, K. Robins, *Nature* **2012**, *485*, 185–194.; (b) J. Turner, M. D. Truppo, *Curr. Opin. Chem. Biol.* **2013**, *17*, 212–214.; (c) P. J. Deuss, R. Denheeten, W. Laan, P. C. J. Kamer, *Chem. Eur. J.* **2011**, *17*, 4680–4698.; (d) T. Ueno, S. Abe, N. Yokoi, Y. Watanabe, *Coord. Chem. Rev.* **2007**, *251*, 2717–2731.; (e) P. K. Sasmal, C. N. Streu, E. Meggers, *Chem. Commun.*, **2013**, *49*, 1581–1587.; (f) M. Martínez-Calvo, J. L. Mascareñas, *Coord. Chem. Rev.* **2018**, *359*, 57–79.

2 (a) K. Yamamura, E. T. Kaiser, *J. Chem. Soc., Chem. Commun.* **1976**, 830–831.; (b) M. E. Wilson, G. M. Whitesides, *J. Am. Chem. Soc.* **1978**, *100*, 306–307.; (c) C.-C. Lin, C.-W. Lin, A. C. S. Chan, *Tetrahedron: Asymmetry* **1999**, *10*, 1887–1893.; (d) O. Pàmies and J. E. Bäckvall, *Chem. Rev.* **2003**, *103*, 3247–3261.; (e) J. C. Lewis, *ACS Catal.* **2013**, *3*, 2954–2975.; (f) Y. Lu, N. Yeung, N. Sieracki, N. M. Marshall, *Nature* **2009**, *460*, 855.

3 (a) D. Montserrat, J. E. Bäckvall, O. Pàmies, *Artificial Metalloenzymes and MetalloDNAzymes in Catalysis: From Design to Applications*, Wiley-VCH, Weinheim, Germany, **2018**., (b) I. Drienovská, C. Mayer, C. Dulson, G. Roelfes, *Nat. Chem.* **2018**, 1., (c) F. Schwizer, Y. Okamoto, T. Heinisch, Y. Gu, M. M. Pellizzoni, V. Lebrun, R. Reuter, V. Köhler, J. C. Lewis, T. R. Ward, *Chem. Rev.* **2018**, *118*, 142–231., (d) S. C. Hammer, A. M. Knight, F. H. Arnold, *Curr. Opin. Green Sustain. Chem.* **2017**, *7*, 23–30., (e) L. Olshansky, R. Huerta-Lavorie, A. I. Nguyen, J. Vallapurackal, A. Furst, T. D. Tilley, A. S. Borovik, *J. Am. Chem. Soc.* **2018**, *140*, 2739–2742., (f) T. Hayashi, Y. Sano, A. Onoda, *Isr. J. Chem.* **2015**, *55*, 76–84.

4 (a) J. Podtetenieff, A. Taglieber, E. Bill, E. J. Reijerse, M. T. Reetz, *Angew. Chem., Int. Ed.* **2010**, *49*, 5151–5155.; (b) J. Bos, G. Roelfes, *Curr. Opin. Chem. Biol.* **2014**, *19*, 135–143.; (c) H. M. Key, P. Dydio, D. S. Clark, J. F. Hartwig, *Nature* **2016**, *534*, 534–537.; (d) P. Dydio, H. M. Key, A. Nazarenko, J. Y.-E. Rha, V. Seyedkazemi, D. S. Clark, J. F. Hartwig, *Science* **2016**, *354*, 102–106.; (e) M. Pellizzoni, G. Facchetti, R. Gandolfi, M. Fusè, A. Contini, I. Rimoldi, *ChemCatChem* **2016**, *8*, 1665–1670.; (f) W. J. Song, F. A. Tezcan, *Science* **2014**, *346*, 1525–1528.; (g) K. Wieszczycka, K. Staszak, *Coord. Chem. Rev.* **2017**, *351*, 160–171.;

5 C. M. Dundas, D. Demonte, S. Park, *Appl. Microbiol. Biotechnol.* **2013**, *97*, 9343–9353.

6 (a) H. Yang, A. M. Swartz, H. J. Park, P. Srivastava, K. Ellis-Guardiola, D. M. Upp, G. Lee, K. Belsare, Y. Gu, C. Zhang, R. E. Moellering, J. C. Lewis, *Nat. Chem.* **2018**, *10*, 318–324.; (b) S. A. Vedha, G. Velmurugan, P. Venuvanalingam, *RSC Adv.* **2016**, *6*, 81636–81646.; (c) D. J. Sommer, M. D. Vaughn, G. Ghirlanda, *Chem. Commun.* **2014**, *50*, 15852–15855.; (d) S. Sahu, L. R. Widger, M. G. Quesne, S. P. de Visser, H. Matsumura, P. Moënne-Loccoz, M. A. Siegler, D. P. Goldberg, *J. Am. Chem. Soc.* **2013**, *135*, 10590–10593.; (e) R. L. Shook, A. S. Borovik, *Inorg. Chem.* **2010**, *49*, 3646–3660.; (f) J.-L. Zhang, D. K. Garner, L. Liang, D. A. Barrios, Y. Lu, *Chem. Eur. J.* **2009**, *15*, 7481–7489.

7 (a) M. Hestericová, T. Heinisch, L. Alonso-Cotchico, J.-D. Maréchal, P. Vidossich, T. R. Ward, *Angew. Chem., Int. Ed.* **2018**, *57*, 1863–1868.; (b) M. Jeschek, R. Reuter, T. Heinisch, C. Trindler, J. Klehr, S. Panke, T. R. Ward, *Nature* **2016**, *537*, 661–665.; (c) V. M. Robles, M. Dürrenberger, T. Heinisch, A. Lledós, T. Schirmer, T. R. Ward, J. D. Maréchal, *J. Am. Chem. Soc.* **2014**, *136*, 15676–15683.; (d) M. Dürrenberger, T. Heinisch, Y. M. Wilson, T. Rossel, E. Nogueira, L. Knörr, A. Mutschler, K. Kersten, M. J. Zimbron, J. Pierron, T. R. Ward., *Angew. Chem., Int. Ed.* **2011**, *50*, 3026–3029.

8 M. M. Pellizzoni, F. Schwizer, C. W. Wood, V. Sabatino, Y. Cotelle, S. Matile, D. N. Woolfson, T. R. Ward, *ACS Catal.* **2018**, *8*, 1476–1484.

9 M. Hestericová, M. R. Correro, M. Lenz, P. F.-X. Corvini, P. Shahgaldian, T. R. Ward, *Chem. Commun.* **2016**, *52*, 9462–9465

10 (a) N. Madern, B. Talbi, M. Salmain, *Appl. Organomet. Chem.* **2013**, *27*, 6–12.; (b) H. Tabe, S. Abe, T. Hikage, S. Kitagawa, T. Ueno, *Chem. As. J.* **2014**, *9*, 1373–1378.; (c) I. W. McNae, K. Fishburne, A. Habtemariam, T. M. Hunter, M. Melchart, F. Wang, M. D. Walkinshaw, P. J. Sadler, *Chem. Commun.* **2004**, 1786–1787.; (d) C. Mayer, D. Hilvert, *European J. Org. Chem.* **2013**, *2013*, 3427–3431.

11 J.-N. Rebilly, B. Colasson, O. Bistri, D. Over, O. Reinaud, *Chem. Soc. Rev.* **2015**, *44*, 467–489.

12 (a) Z. Wang, Y. Takezawa, H. Aoyagi, S. Abe, T. Hikage, Y. Watanabe, S. Kitagawa, T. Ueno, *Chem. Commun.* **2011**, *47*, 170–172.; (b) S. Abe, K. Hirata, T. Ueno, K. Morino, N. Shimizu, **2009**, 6958–6960.; (c) S. Abe, J. Niemeyer, M. Abe, Y. Takezawa, T. Ueno, T. Hikage, G. Erker, Y. Watanabe, *J. Am. Chem. Soc.* **2008**, *130*, 10512–10514.; (d) T. Ueno, M. Suzuki, T. Goto, T. Matsumoto, K. Nagayama, Y. Watanabe, *Angew. Chemie - Int. Ed.* **2004**, *43*, 2527–2530.

13 (a) F. Schwizer, V. Köhler, M. Dürrenberger, L. Knörr, T. R. Ward, *ACS Catal.* **2013**, *3*, 1752–1755.; (b) H. Mallin, M. Hestericová, R. Reuter, T. R. Ward, *Nat. Protoc.* **2016**, *11*, 835–852.; (c) Y. Okamoto, V. Köhler, C. E. Paul, F. Hollmann, T. R. Ward, *ACS Catal.* **2016**, *6*, 3553–3557.

14 (a) M. Gerl, R. Jaenicke, *Eur. Biophys. J.* **1987**, *15*, 103–109.; (b) M. Kim, Y. Rho, K. S. Jin, B. Ahn, S. Jung, H. Kim, M. Ree, *Biomacromolecules* **2011**, *12*, 1629–1640.

15 (a) D. Belletti, F. Pederzoli, F. Forni, M. A. Vandelli, G. Tosi, B. Ruozi, *Expert Opin. Drug Deliv.* **2017**, *14*, 825–840.; (b) Wang, C. Zhang, L. Liu, Z. Li, F. Guo, X. Li, J. Luo, D. Zhao, Y. Liu, Z. Su, *J. Biotechnol.* **2017**, *254*, 34–42.; (c) J. Zang, H. Chen, G. Zhao, F. Wang, F. Ren, *Crit. Rev. Food Sci. Nutr.* **2017**, *57*, 3673–3683.; (d) J. Chen, G. C. Zhao, *Talanta* **2017**, *168*, 62–66.; (e) G. Jutz, P. Van Rijn, B. Santos Miranda, A. Böker, *Chem. Rev.* **2015**, *115*, 1653–1701.; (f) K. W. Pulsipher, I. J. Dmochowski, *Isr. J. Chem.* **2016**, 1–12.; (g) L. Turyanska, T. D. Bradshaw, J. Sharpe, M. Li, S. Mann, N. R. Thomas, A. Patanè, *Small* **2009**, *5*, 1738–1741.

16 (a) Z. Heger, S. Skalickova, O. Zitka, V. Adam, R. Kizek, *Nanomedicine* **2014**, *9*, 2233–2245.; (b) X. Li, L. Qiu, P. Zhu, X. Tao, T. Imanaka, J. Zhao, Y. Huang, Y. Tu, X. Cao, *Small* **2012**, *8*, 2505–2514.